High affinity of 3D spongin scaffold towards Hg(II) in real waters.

Eddy M. Domingues[a*], Gil Gonçalves[a*], Bruno Henriques[b,c], Eduarda Pereira[c] and Paula A. A. P. Marques[a*]

[a] - TEMA, Mechanical Engineering Department, University of Aveiro, 3810-193 Aveiro, Portugal

[b] - CESAM & Department of Chemistry, University of Aveiro, 3810-193 Aveiro, Portugal

c - LAQV-REQUIMTE, Department of Chemistry & Central Laboratory of Analysis, University of Aveiro, 3810-193 Aveiro, Portugal

Supplementary Information

The 3D spongin scaffold samples used in this paper were cleaned by mechanically pressing the samples under distilled water and leaving the samples under magnetic agitation in 2 L of distilled water for 24h (2 times), as described in the Materials and Methods section of the manuscript. To elucidate the chemical composition of the MS samples before and after the cleaning protocol we performed EDS on the as-received (Figure SI-1A) and cleaned (Figure SI-1B) spongin scaffold. One can see that the received materials have some impurities, mainly observed by the presence of Ca, F, Cl, Na, K, S and Mn, most probably as inorganic compounds. The EDS spectra and mapping of the cleaned MS samples showed a dramatically reduced intensity of Ca and S peaks and the almost total removal of F, Cl, Na, K and Mn.

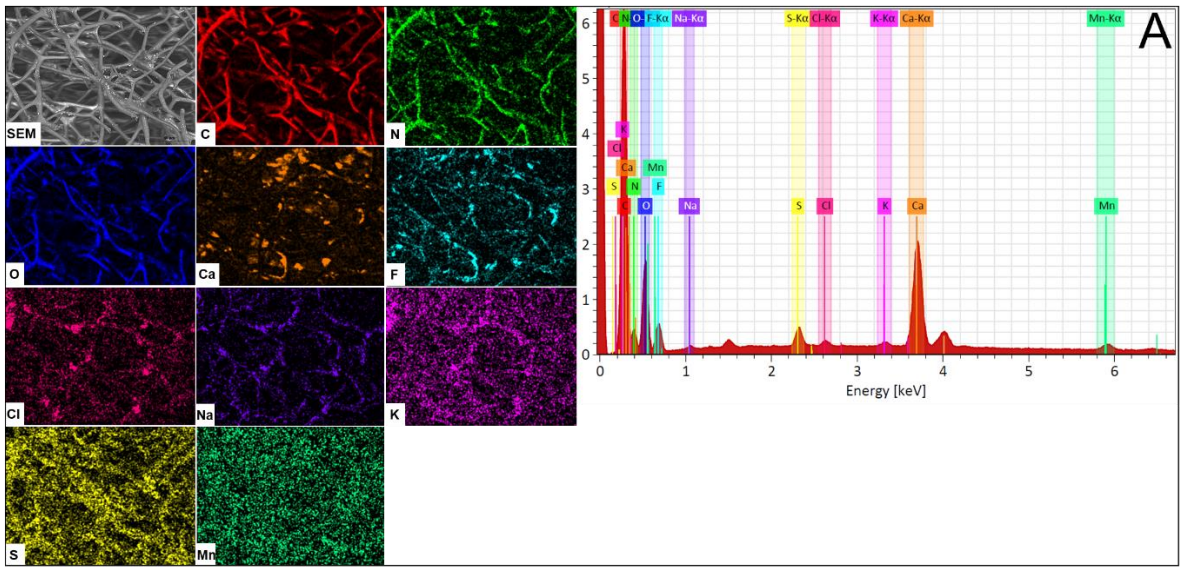

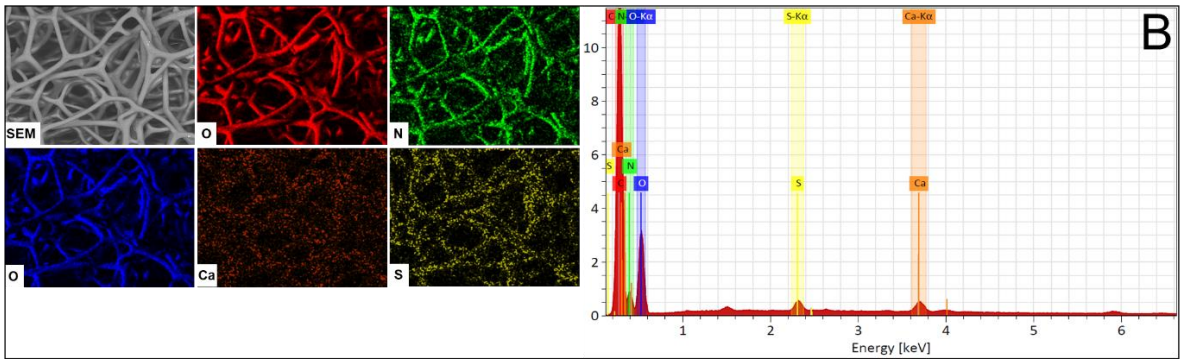

Figure SI-1. EDS analysis of the A) as-received and B) cleaned MS samples used in this study.

Table SI-1. Elemental analysis of the bottled water matrix (Fastio®) used in the study

Bottled water (Fastio®) Initial pH = 5.9			
Major elements (mg L^{-1})		*Minor elements* (µg L^{-1})	
Ca	1.3	B	20
Na	4.1	Al	50
K	0.6	Cr	1.3
Mg	0.7	Fe	61
P	0.4	Co	< 1
Si	0.8	Ni	< 1
Cl	4.2	Cu	3.1
		Zn	20
		As	< 2
		Se	< 1
		Sr	6.3
		Cd	<0.1
		Sb	< 0.1
		Ba	3.1
		Pb	< 0.1

Table SI.2 is a collection of the mathematical equation used in the kinetic modelling of the sorption data. q_t is the amount of metal sorbed per gram of at time t (µmol g^{-1}), q_e amount of metal adsorbed per gram of materials at equilibrium (µmol g^{-1}), k_1 rate constant of pseudo-first order (h^{-1}), k_2 rate constant of pseudo-second order (g µmol^{-1} h^{-1}), α initial sorption rate (µmol g^{-1} h^{-1}), β desorption constant (g µmol^{-1}).

Table SI-2. Sorption reaction kinetic models

Kinetic model	Equation	References
Pseudo-first-order (Lagergren)	$q_t = q_e(1-e^{-k_1 t})$	[1]
Adsorption capacity Pseudo-second-order (Ho)	$q_t = \frac{q_e^2 k_2 t}{1+q_e k_2 t}$	[2]
Elovich	$q_t = \frac{1}{\beta}\ln(1+\alpha\beta t)$	[3]

We also applied two extensively known diffusion-based models, Boyd's film-diffusion [4] and Webber's pore-diffusion [5], to study the sorption mechanism and which rate-controlling step is drives the sorption process.

In the film-diffusion model presented by Boyd, the main opposition to diffusion is in the boundary layer surrounding the adsorbent particle[6,7], expressed as:

$$F = 1 - \frac{6}{\pi^2}\sum_{n=1}^{\infty}\left(\frac{1}{n^2}\right)\exp\left(-n^2 Bt\right) \quad (4)$$

where F is the fractional attainment of equilibrium, at different times, t, and Bt is a function of F:

$$F = \frac{q_t}{q_e} \quad (5)$$

Bt can be calculated as:

For F values > 0.85 $$Bt = -0.4977 - \ln\left(1 - F\right) \quad (6)$$

For F values < 0.85 $$Bt = \left(\sqrt{\pi} - \sqrt{\pi - \frac{\pi^2 F}{3}}\right)^2 \quad (7)$$

If the Boyd's plot (Bt vs t) excludes the origin, the film diffusion or chemical reaction must be the rate-controlling step, whereas if the plot is linear and passes through the origin, it is the intra-particle diffusion that mostly controls the rate of mass transfer.

Weber's intraparticle-diffusion model is defined by the equation [6,7] :

$$q_t = k_i t^{1/2} \quad (8)$$

In which ki is the intraparticle-diffusion parameter (mg g^{-1} $h^{-1/2}$). If a plot of qt vs t is a straight line with a slope that equals ki and an intercept equal to zero, the intraparticle-diffusion must be the rate-limiting step. If not, there must be another mechanism along with intraparticle diffusion must be considered. To analyse the experimental data under

77 the film-diffusion and the intraparticle-diffusion models, and to predict the corresponding
78 diffusion coefficients, a piecewise linear regression methodology (PLR), proposed by
79 Malash et al. [6], was performed using a Microsoft® Excel™ worksheet developed by
80 these authors.
81
82 In Table SI-3 one can find the equation that described the several equilibrium models
83 applied, where, q_m is the maximum sorption capacity (mg g^{-1}), b_L is the Langmuir
84 constant related to the free energy of adsorption (L mg^{-1}), C_e is the concentration of
85 metal sorbed in the equilibrium μg. L^{-1}, K_F is a constant related to the adsorption
86 capacity of the sorbent ($mg^{1-1/n}$ $L^{1/n}$ g^{-1}) and *n* is the adsorption intensity or the
87 heterogeneity of the sorbent, β (mol^2 kJ^{-2}) is a constant related to the adsorption energy,
88 b is the variation of adsorption energy (kJ mol^{-1}), K_t is the Temkin equilibrium constant
89 (L mg^{-1}), and b_S is the Sips constant related to the energy of adsorption (L $mg^{-1})^{1/n}$.

90 Table SI-3. Sorption reaction kinetic models

Equilibrium model	Equation	References
Freunlich isotherm	$q_e = K_F C_e^{1/n}$	[8]
Langmuir isotherm	$q_e = \frac{q_m b_L C_e}{1 + b_L C_e}$	[8]
Dubinin-Radushkevich	$q_e = q_m e^{\left(-K_e R T \ln\left(1+\frac{1}{C_e}\right)\right)^2}$	[9]
Temkin	$q_e = \frac{R T}{b} \ln(K_t C_e)$	[8]
Sips	$q_e = \frac{q_m (b_S C_e)^{1/n}}{1 + (b_S C_e)^{1/n}}$	[10]

91
92

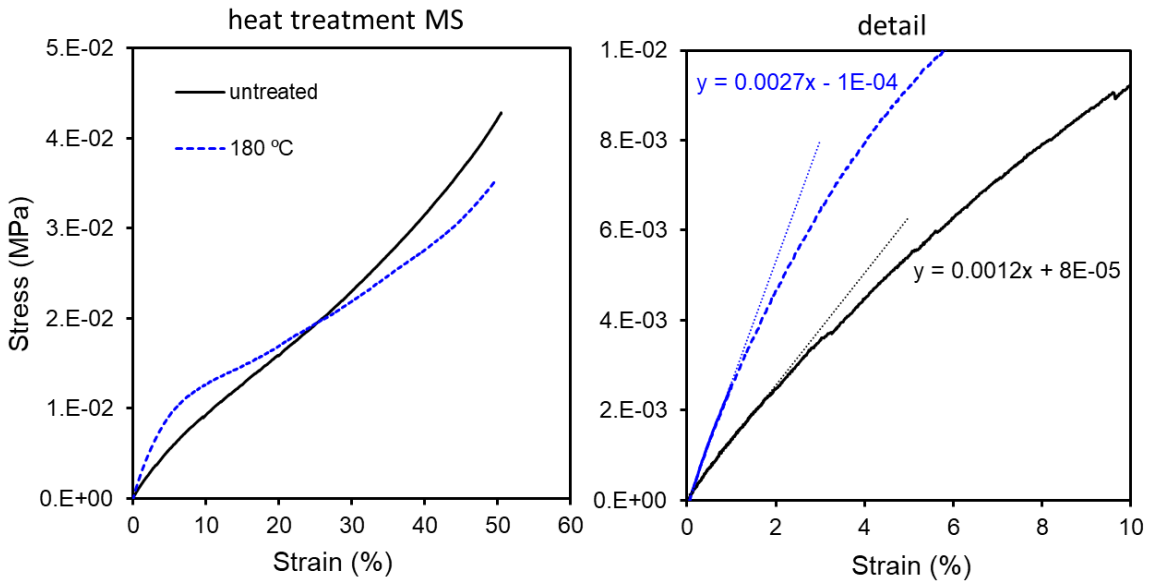

Figure SI-2. Mechanical test (stress-strain) curves on a sample of MS before and after a heat-treatment at 180 ºC. The plots show an increase in stiffness, corresponding to an increase in Young's modulus from 120 kPa to 270 kPa after the heat treatment.

Table SI-4. Kinetic parameters resulting from the application of Weber's intraparticle-diffusion model.

Matrix	stag	Breakpoint	K_i (µg g^{-1} h^{-}	R^2
MQ	1	76	107.2	0.9824
	2	-	3.242	0.8955
bottled	1	77	94.98	0.9508
	2	-	2.943	0.9145
sea	1	164	55.76	0.9359
	2	-	7.882	0.9124

References

[1] S. Lagergren, About the theory of so-called adsorption of soluble substances, K. Sven Veten Hand. 24 (1898) 1–39.

[2] Y.S. Ho, G. McKay, Pseudo-second order model for sorption processes, Process Biochem. 34 (1999) 451–465. https://doi.org/Doi 10.1016/S0032-9592(98)00112-5.

[3] M.J.D. Low, Kinetics of Chemisorption of Gases on Solids, Chem. Rev. 60 (1960) 267–312. https://doi.org/Doi 10.1021/Cr60205a003.

[4] G.E. Boyd, A.W. Adamson, L.S. Myers, The Exchange Adsorption of Ions from Aqueous Solutions by Organic Zeolites .2., J. Am. Chem. Soc. 69 (1947) 2836–2848. https://doi.org/Doi 10.1021/Ja01203a066.

[5] W.J. Weber, J.C. Morris, Kinetics of adsorption on carbon from solution, Kinet. Adsorpt. Carbon from Solut. (1963).

[6] G.F. Malash, M.I. El-Khaiary, Piecewise linear regression: A statistical method for the analysis of experimental adsorption data by the intraparticle-diffusion models, Chem. Eng. J. 163 (2010) 256–263. https://doi.org/10.1016/j.cej.2010.07.059.

[7] Y.S. Ho, J.C.Y. Ng, G. McKay, Kinetics of pollutant sorption by biosorbents: Review, Sep. Purif. Methods. 29 (2000) 189–232. https://doi.org/10.1081/SPM-100100009.

[8] O. Hamdaoui, E. Naffrechoux, Modeling of adsorption isotherms of phenol and chlorophenols onto granular activated carbon. Part I. Two-parameter models and equations allowing determination of thermodynamic parameters, J. Hazard. Mater. 147 (2007) 381–394. https://doi.org/10.1016/j.jhazmat.2007.01.021.

[9] Q. Hu, Z. Zhang, Application of Dubinin–Radushkevich isotherm model at the solid/solution interface: A theoretical analysis, J. Mol. Liq. 277 (2019) 646–648. https://doi.org/10.1016/j.molliq.2019.01.005.

[10] R. Sips, On the structure of a catalyst surface, J. Chem. Phys. 16 (1948) 490–495. https://doi.org/10.1063/1.1746922.